Articles

Distribution of the Chlorophyll Spectral Forms in the Chlorophyll–Protein Complexes of Photosystem II Antenna

Robert C. Jennings,*,‡ Roberto Bassi,§ Flavio M. Garlaschi,‡ Paola Dainese,§ and Giuseppe Zucchelli‡

Centro CNR Biologia Cellulare e Molecolare delle Piante, Dipartimento di Biologia, Universita' di Milano, via Celoria 26, 20133 Milano, Italy, and Dipartimento di Biologia, Universita' di Padova, via Trieste 75, 35121 Padova, Italy

Received September 29, 1992; Revised Manuscript Received January 14, 1993

ABSTRACT: The chlorophyll–protein complexes that form the antenna system of photosystem II have been purified and analyzed in terms of the commonly observed chlorophyll spectral forms. With the exception of chlorophyll *b*, which is known to be associated with the complexes comprising the outer antenna (LHCII, CP24, CP26, CP29), the spectral forms occur with similar absorption maxima and are present in rather similar amounts in each of the antenna complexes. On the basis of the published chlorophyll stoichiometries for the complexes in photosystem II antenna, the distribution of the spectral forms in a "reconstituted" antenna has been determined. These data were used to calculate the equilibrium population of excited states within the various chlorophyll–protein complexes within photosystem II. This was compared with the light absorption capacity of each of the complexes in the "reconstituted" antenna. The ratio of these two parameters (excited-state equilibrium distribution/absorption capacity) was determined to be 1.21 for the inner (core) antenna and 0.88 for LHCII. The standard free energy change for exciton transfer from the outer to the inner antenna was calculated to be –0.17 kcal mol^{-1}. It is concluded that the photosystem II antenna is arranged as a very shallow funnel.

The absorption of radiant energy by the photosystems of green plants is achieved by a large array of antenna pigments of which the chlorophylls are of paramount importance. For higher plant photosystem II, there are about 200–250 antenna chlorophyll (chl)[1] molecules for every RC[1] (Anderson, 1986). Excitation energy is transferred with high efficiency from the antenna array to RCs where charge separation occurs. While the single chl–chl transfer rates are not known with any certainty, it is often suggested that they are on a picosecond time scale [e.g., see Gillbro et al. (1988)]. The overall RC trapping time (primary charge separation) in PS II has been recently determined to be around 300 ps (Leibl et al., 1990), thus indicating a large number of energy-transfer steps prior to trapping.

It has become increasingly evident in recent years that the antenna system of higher plant PS II is extremely heterogeneous at several different levels. One such level pertains to the different chl–protein complexes which constitute the physical structure of the antenna. Thus, at least six different antenna complexes are currently recognized (Bassi et al., 1990). Two of these are the so-called inner (core) antenna complexes CP43 and CP47 which contain only chl *a* and are thought to be closely associated with the RC complex. The outer antenna is made up of one major (LHCII) and three minor complexes (CP24, CP26, and CP29), all of which contain both chl *a* and chl *b*. About 60% of the total PS II antenna chl is usually associated with LHCII (Anderson, 1980) which appears to be structurally and functionally heterogeneous (Kyle et al., 1984; Jennings et al., 1986; Spangfort & Anderson, 1989). Largely on the basis of detergent fractionation studies, several attempts have been made to describe the topological organization of these complexes within the PS II antenna system (Bassi et al., 1987; Dainese & Bassi, 1991; Peter & Thornber, 1991). It has not been possible, however, to relate these structural antenna models to energy transfer within the antenna due to lack of knowledge on the distribution of the chlorophyll spectral forms within the complexes.

Another level of antenna heterogeneity concerns the spectroscopic characteristics of the chl antenna pigments. Thus, at least five distinct chl *a* spectral forms have been detected in PS II antenna by derivative spectroscopy and Gaussian band decomposition of low-temperature absorption spectra (French et al., 1972; Brown & Schoch, 1981; Van Dorssen et al., 1987b) and by Gaussian analysis of room temperature spectra (Van Ginkel & Kleinen-Hammans, 1981; Zucchelli et al., 1990). The absorption maxima (Q_y transition) of these spectral forms are approximately at 660, 670, 678, 684, and 695 nm. It is generally assumed that these spectral bands represent separate electronic (Q_y) transitions of different chl *a* forms present in photosynthetic antenna systems. Chl *b*, which seems to be present as a single spectral band, usually absorbs maximally (Q_y transition) near 648 nm. It has recently been demonstrated (Zucchelli et al., 1992) that each of these spectral forms has a characteristic fluorescence emission spectrum which can be well described by asymmetric Gaussian bands. On the basis of a detailed analysis of the spectral characteristics of fluorescence quenching by open RCs, it has been suggested that these spectral forms transfer energy to RCs with differences in average efficiency (Jennings et al.,

* Address correspondence to this author.
‡ Universita' di Milano.
§ Universita' di Padova.

[1] Abbreviations: BBY-grana, grana prepared as described by Berthold et al. (1981); chl, chlorophyll; chl$^{n}_{m}$, chlorophyll spectral form with absorption and emission maxima at *n* and *m* nm, respectively; CP, chlorophyll–protein complex; DM, dodecyl maltoside; FWHM, full width at half-maximum; IEF, isoelectric focusing; LHCII, light-harvesting chlorophyll *a*/*b* protein complex II; PS II, photosystem II; RC, reaction center.

0006-2960/93/0432-3203$04.00/0

1990, 1991). In this sense, chl^{684}, followed by chl^{678}, displays the highest transfer efficiency to RCs with progressively decreasing efficiencies for both longer and shorter wavelength bands. These observations can be most simply interpreted in terms of a "funnel" organization of the antenna pigments with the chl^{684} and chl^{678} forms being concentrated within the core antenna, in close proximity to the RCs, and the shorter wavelength pigments being present at relatively high concentrations in the external antenna. This interpretation, however, was shown to be inadequate as the chl^{684} form is present at quite high levels in the principal outer antenna complex LHCII (Zucchelli et al., 1990) and does not seem to be concentrated in the core antenna (Jennings et al., 1990). In addition, it has been recently demonstrated by steady-state emission analysis that excitation energy does not seem to be concentrated in the core antenna prior to fluorescence emission (Jennings et al., 1991).

In order to further understand the role of antenna heterogeneity in energy transfer to PS II RCs, it is necessary to document the distribution of the chl spectral forms within the various antenna complexes. While van Dorssen et al. (1987a,b) have described the spectral forms present in CP47 and the PS II core at 4 K and Zucchelli et al. (1990) and Jennings et al. (1990) have studied the LHCII spectral forms at both room temperature and 77 K, no systematic attempt at such an analysis has been reported. In the present paper, we report such a study. All measurements were performed at room temperature as it has been demonstrated that low temperatures lead to the loss of chl^{684} in LHCII (Zucchelli et al., 1990). The data demonstrate the presence of all the chl *a* spectral forms in each antenna complex. On the basis of the thermal equilibrium assumption, we have calculated the excited-state distribution between chl forms in the various complexes and the standard free energy change for excited-state transfer from the outer to the inner antenna. It is concluded that the PS II antenna is arranged as an extremely shallow funnel.

MATERIALS AND METHODS

Preparation of Thylakoid Membranes. Seedlings of Zea mays (cv Dekalb DF28) were grown for 2–3 weeks in a growth chamber at 12 h/12 h light/dark and 28/21 °C day/night at a light intensity of 10000 lux and 80% humidity. Leaves from 2–3-week-old plants were harvested at the end of a 12-h dark period, and thylakoids from mesophyll chloroplasts were obtained as previously described (Bassi & Simpson, 1986). PS II membranes were prepared according to the method of Berthold et al. (1981), using the modifications described by Dunahay et al. (1984). Aliquots were resuspended at 3 mg of chl/mL in 25 mM Hepes, pH 7.6, 5 mM $MgCl_2$, 10 mM NaCl, and 0.2 M sorbitol and frozen at −80 °C until required.

Sucrose Gradient Ultracentrifugation. PS II membranes were washed twice in 1 mM EDTA, pH 8.0, then resuspended in water at 2 mg of chl/mL, and solubilized by adding an equal volume of 2% DM in water. When required, other detergent concentrations were used or $MgCl_2$ was added to a final concentration of 5 mM, in both the solubilization mixture and the sucrose gradient. The solubilized sample was spun for 2 min at 15000*g* at 4 °C and then rapidly loaded onto a 0.1–1.0 M sucrose gradient containing 10 mM Hepes, pH 7.6, and 0.06% DM. The gradient was then spun on a Beckman SW41 rotor at 39 000 rpm for 23 h at 4 °C. For quantitative determinations, the gradient was fractionated from the top into 250-μL aliquots.

Photosystem II Core Preparation. PS II preparations, depleted of LHCII, were obtained according to Ghanotakis et al. (1987). The PS II core complex, binding only chl *a*, was prepared by sucrose gradient ultracentrifugation as described above. The most mobile band was collected and loaded onto a flat-bed IEF gel to eliminate contamination with chl *a*/*b* binding proteins (Dainese et al., 1990). PS II was collected as a diffuse green band at p*I* 5.2. The complete removal of chl *a*/*b* proteins was assessed by immunoblot with anti-CAB antibodies.

Purification of chl a/b Binding Proteins. Purified LHCII, CP29, CP26, and CP24 were obtained as previously reported (Dainese et al., 1990; Bassi & Dainese, 1992; Dainese & Bassi, 1991).

Purification of CP43 and CP47. PS II chl *a* binding proteins were obtained by fractionating the PS II core preparation from sucrose gradient ultracentrifugation, by ion-exchange chromatography as described by Dekker et al. (1989). This procedure yielded CP43 contaminated with small amounts of LHCII, which were removed by flat-bed IEF (Dainese et al., 1990).

SDS–PAGE and Immunoblotting. Analytical SDS–PAGE was performed with gradient gels (12–18% acrylamide, 350 × 350 × 1 mm) containing 6 M urea and run at 10 mA for 3 days using the Tris–sulfate buffer system as previously described (Bassi et al., 1987). Alternatively, a high-Tris buffer system with urea (12–18% acrylamide gradient) was used (Fling & Gregerson, 1986). For immunoblot, assay samples were separated by one of the gel systems described above and transferred to a nitrocellulose filter (Millipore, Bedford). The filters were then assayed with antibodies, and antibody binding was detected by using alkaline phosphatase coupled to anti-rabbit IgG (Sigma Chemical Co.). Antibodies were raised in rabbits and characterized as previously described (Di Paolo et al., 1990).

Spectroscopic Analysis. Absorption spectra of the various complexes were measured using an EG&G OMAIII (Model 1460) with an intensified diode array (Model 1420) mounted on a spectrograph (Jobin-Yvon HR320) with a 150 groove mm^{-1} grating. The wavelength scale of the instrument was calibrated using a neon spectral calibration source (Cathodeon). The wavelength spacing between pixels is about 0.5 nm. The incident light from a halogen lamp was passed through an 560LP filter (Ditric Optics) and attenuated by neutral filters. An OG530 filter (Schott) was placed before the collection optics to eliminate stray light; the sample was contained in a 1-mm path-length cuvette with an opal glass placed behind to substantially eliminate scattering artifacts, and the residual absorption at 750 nm was subtracted from the spectra. The chl–protein complexes were diluted at the chl concentration of about 10 μg/mL, giving a maximum Q_y absorbance of about 25 × 10^{-3}, with Hepes buffer (10 mM, pH 7.6) which contained, depending on the experiment, 0.06% DM.

Curve Fit Procedure. Decomposition analysis of the spectra in terms of "asymmetric" Gaussian bands was performed as already described (Zucchelli et al., 1990) using a nonlinear least-squares algorithm that minimizes the χ^2 function with respect to the parameters of a model function. This model function is written as the sum of a variable number (maximum number 20) of "asymmetric" Gaussian curves. In all fits, the band parameters were left free. As each band has four independent parameters (the wavelength position, the height, and the two FWHM), the fits were performed over a hypersurface in a multidimensional space in which the search for a minimum could, in principle, be complicated by the presence of more than one minimum that might also be broad.

We have therefore stipulated that the major bands in the fit must not display a pronounced asymmetry toward longer wavelengths. This is physically well founded for chlorophyll in nonpolar solvents (Shipman et al., 1976; Reddy et al., 1992). Initial conditions regarding the number and position of the main Gaussian bands were chosen on the basis of the second-derivative analysis of absorption spectra (unpublished data). The choice of different initial band numbers and/or positions gave rise to fits which either converged on those obtained as described above or else were statistically less good. When a satisfactory minimum was obtained, subsequent iteration gave only minor changes in the parameters, thus indicating that the minima are not wide.

We have also estimated the uncertainties associated with the fit parameters. These were obtained by calculating the error matrix using a parabolic approximation. The error matrix was obtained as the inverse of the curvature matrix, i.e., the second-derivative matrix of the χ^2 function with respect to its free parameters, evaluated at the best parameter values (the function minimum). The diagonal elements of the error matrix are the squares of the errors of each parameter together with the effect of correlations with the other parameters. The curvature matrix of the χ^2 function has, as diagonal elements, the second partial derivatives with respect to each parameter. These elements are therefore not coupled to the other parameters, but when the matrix is inverted, the diagonal elements of the inverse contain contributions from all the elements of the second-derivative matrix (Bevington, 1969). These errors, that are symmetric due to the parabolic approximation, are those reported in Table I. Their meaning is that if a parameter is changed by a value equivalent to its error, the χ^2 value increases by 1. Thus, the errors indicate the width of the minima.

Other Methods. Chlorophyll and carotenoid determinations were made in 80% acetone using the equations of Wellburn and Lichtenthaler (1983) or Porra et al. (1989). The two methods yielded very similar results for chl *a* to chl *b* ratios ranging from 1 to 3. Protein determination in solution was by the bicinchoninic acid method (Smith et al., 1985). DM was substantially removed from the complexes, when required, by a 20-fold dilution with Hepes buffer (10 mM, pH 7.6) followed by 16-h ultracentrifugation in a Beckman SW 50.1 rotor at 45 000 rpm at 4 °C. The precipitated complexes were resuspended in the same buffer.

RESULTS

Polypeptide Composition of the Chlorophyll–Protein Complexes. The polypeptide composition of the chlorophyll–protein complexes isolated as described under Materials and Methods is shown in Figure 1, as analyzed by SDS–urea–PAGE. The PS II core system contains the CP47, CP43, D1, D2, and cytochrome *b*-559 polypeptides. D1 and D2, besides their location in the 30-kDa region of the gel, also appear at around 60 kDa in the heterodimer aggregation form. In lane 2 of Figure 1, the CP47 preparation shows two closely migrating bands. Both these bands are recognized by antibodies directed against CP47 (data not shown), thus suggesting that they represent the same protein in two conformations stabilized under our electrophoretic conditions. The polypeptide compositions of CP43 and also of the chlorophyll *a*/*b* proteins (lanes 3–7) are identical to previously described preparations (Dainese & Bassi, 1991; Nanba & Satoh, 1987).

Effect of Dodecyl Maltoside on Light Absorption by chl–Protein Complexes. In order to determine the distribution of

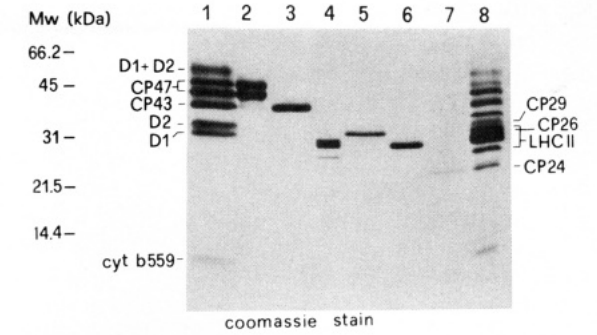

FIGURE 1: SDS–urea–PAGE of the chlorophyll binding preparations from PS II membranes. Lane 1, PS II core complex; lane 2, CP47; lane 3, CP43; lane 4, LHCII; lane 5, CP29; lane 6, CP26; lane 7, CP24; lane 8, PS II membrane.

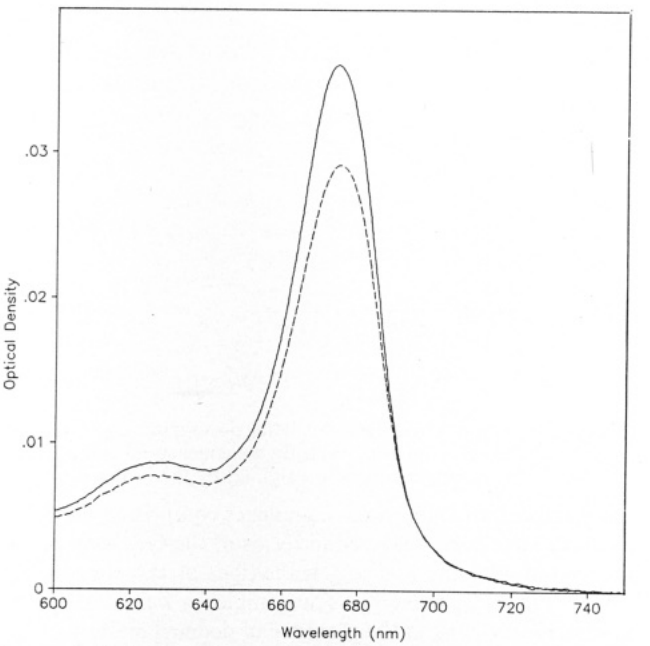

FIGURE 2: Influence of incubation of the photosystem II core complex with dodecyl maltoside on the absorption spectrum. Continuous line, with dodecyl maltoside (0.06%); dashed line, without dodecyl maltoside.

the chl spectral forms among the PS II chl–protein complexes, we have measured the room temperature absorption spectra of the DM-solubilized complexes. As detergent treatment may modify the spectral characteristics, we have initially investigated the effect of 0.06% DM on absorption. In all cases, the detergent brought about a significant increase in optical density which varied between 20% and 40% at the absorption peak. An example of this is presented in Figure 2 for the PS II core preparation. The effect is greatest at the peak and decreases progressively at longer and shorter wavelengths, with decreasing optical density. These absorption effects are characteristic of the so-called "sieve effect" (Duysens, 1956; Latimer, 1983) which occurs when chromophores are present in large aggregates or particles. We therefore believe that dodecyl maltoside brings about the absorption increase by disrupting the aggregation of chl–protein complexes which occurs when they are resuspended in the absence of detergent.

In no case did dodecyl maltoside lead to significant changes in the absorption bands associated with the spectral forms (data not presented).

Distribution of the Chlorophyll Spectral Forms in the chl–Protein Complexes. The room temperature absorption spectra

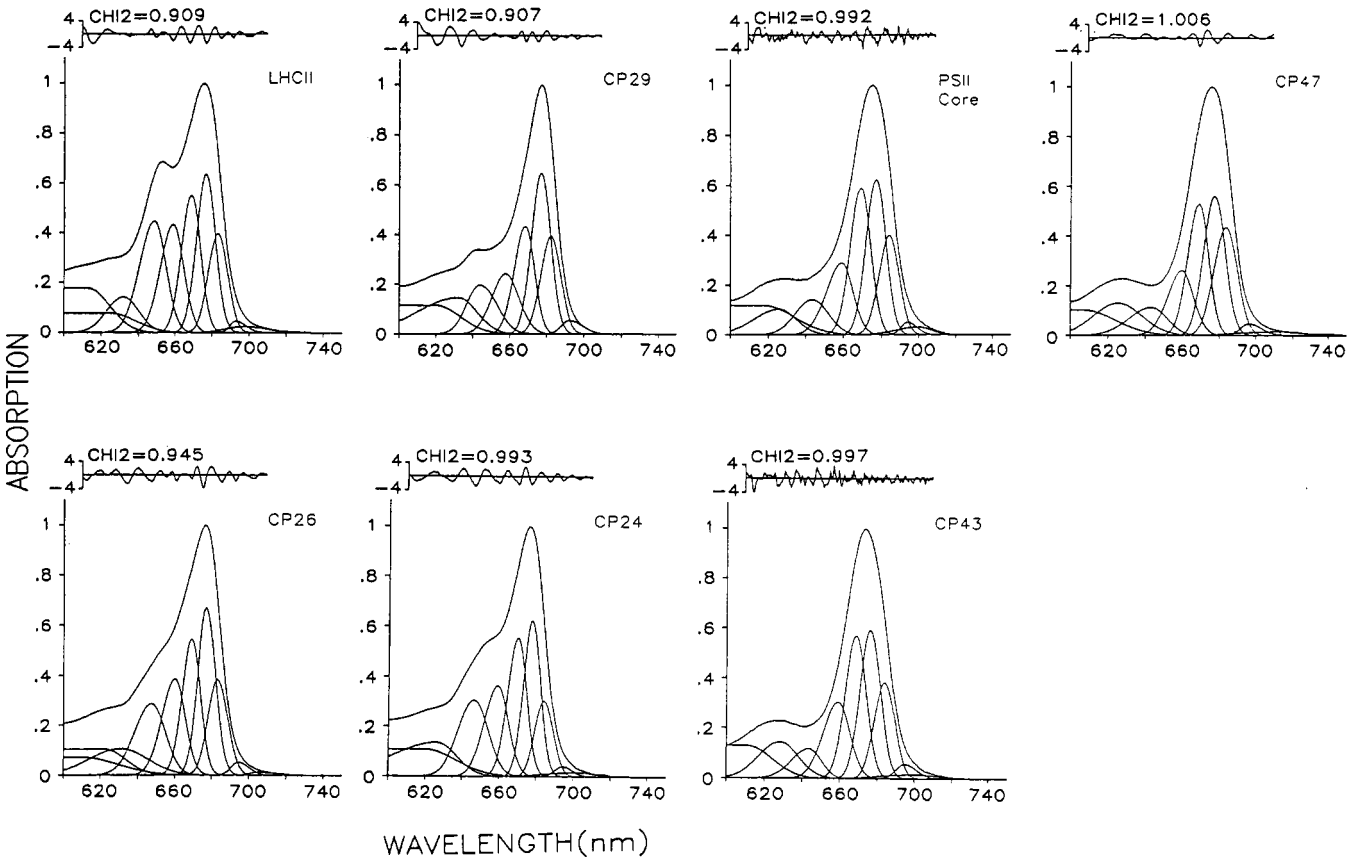

FIGURE 3: Asymmetric Gaussian band decomposition of the room temperature absorption spectra of the chlorophyll–protein complexes comprising the PS II antenna. Spectra were measured in the presence of dodecyl maltoside (0.06%). The residuals are the differences between measured and calculated spectra weighted by the errors of the optical density measurements. The reduced χ^2 values are also shown.

of all the known chl–protein complexes comprising the PS II antenna have been analyzed in terms of the Gaussian bands associated with the main Q_y transitions of the chl spectral forms (Figure 3, Table I). The complexes were purified by isoelectric focusing in the presence of dodecyl maltoside and their spectra measured in the presence of 0.06% of this detergent. These spectra with the relative Gaussian bands are presented in Figure 3, along with the relevant reduced χ^2 and residuals distributions. The fit parameter errors are presented in Table I (see Materials and Methods). The fits presented here are the only reasonable ones possible based on the criteria described under Materials and Methods. The errors indicate that each fit minimum is rather narrow. Inspection of the data indicates the following:

(1) With the exception of chl *b* (648 nm), which is absent in the core complexes (PS II core, CP43, CP47), the various spectral forms are present in all chl–protein complexes. The peak positions and half-bandwidths are rather similar in all cases.

(2) The presence of long-wavelength spectral bands, particularly that with a maximum near 684 nm, previously reported for Triton-X-solubilized LHCII, is here confirmed for the dodecyl maltoside solubilized complex. As reported previously (Zucchelli et al., 1990), the fit is significantly less good if this band is omitted (unpublished observation).

(3) In CP29, the spectral band associated with chl *b* is blue-shifted by about 4 nm with respect to the other complexes (644 nm instead of 648 nm).

(4) The relative absorption contribution of the chl *a* forms is generally somewhat greater in the core antenna with respect to the outer antenna complexes (LHCII, CP24, CP26, CP29) due mainly to the presence of chl *b* in the latter complexes and its absence from the core antenna.

In order to understand the contribution of each spectral form in each chl–protein complex to the overall absorption by the PS II antenna, it is necessary to multiply the Gaussian decomposition for each complex by an appropriate weighting factor. The weighting factors (L_i) were established using the stoichiometric data of Dainese and Bassi (1991) for chl *a* in the PS II complexes (LHCII, 0.51; PS II core, 0.33; CP24, 0.03; CP26, 0.06; CP29, 0.07) and were determined by

$$L_i = \frac{[\text{chl } a]_i 100}{\sum_j A_j}$$

with the normalization condition $\sum_i L_i = 1$, where i represents the different PS II complexes and j the different chl *a* forms. A_j is the absorption of each chl *a* spectral form, and $[\text{chl } a]_i$ is the normalized chl *a* concentration in the different chl–protein complexes. The underlying assumption of this approach is that the extinction coefficients of the chl *a* spectral forms are equal. In this analysis, we have considered the PS II core complex and not its main components CP43 and CP47. The data are presented in Table II. In order to check the validity of our approach, we have compared the absorption spectrum of the "reconstituted" antenna with the measured absorption spectrum of the PS II membrane preparation from maize which was used as the starting material for the purification of the chl–protein complexes. The "reconstituted" antenna was calculated by multiplying the individual absorption spectra of the complexes by the appropriate weighting factor (L_i). This "reconstituted" spectrum is compared with the measured PS II membrane spectrum in Figure 4. Quite good agreement between the two spectra is obtained, thus providing a strong justification for our approach.

Table I: Gaussian Parameters for the Decomposition of the Room Temperature Absorption Spectra of Different Chlorophyll–Protein Complexes Constituting the PS II Antenna[a]

	LHCII	CP29	CP26	CP24	PS II	CP47	CP43
(1) λ_{max} (nm)	649.25 ± 0.09	644.50 ± 0.14	647.93 ± 0.10	647.04 ± 0.12			
FWHM	16.77 ± 0.17	19.00 ± 0.27	19.46 ± 0.21	18.93 ± 0.23			
	9.41 7.36	8.50 10.50	10.67 8.79	10.02 8.90			
% area	22.29 ± 0.35	13.84 ± 0.30	18.24 ± 0.28	20.28 ± 0.38			
(2) λ_{max} (nm)	659.38 ± 0.10	658.00 ± 0.12	660.50 ± 0.08	659.48 ± 0.11	659.63 ± 0.10	660.36 ± 0.13	659.54 ± 0.08
FWHM	14.82 ± 0.19	17.50 ± 0.24	14.80 ± 0.16	15.26 ± 0.21	16.57 ± 0.25	16.85 ± 0.29	16.80 ± 0.18
	8.00 6.82	8.55 8.95	8.21 6.59	8.15 7.11	9.50 7.07	9.17 7.68	9.11 7.69
% area	19.14 ± 0.36	15.70 ± 0.33	18.58 ± 0.29	19.38 ± 0.38	18.95 ± 0.34	17.04 ± 0.40	20.04 ± 0.29
(3) λ_{max} (nm)	669.23 ± 0.08	669.00 ± 0.07	669.55 ± 0.06	670.37 ± 0.07	669.78 ± 0.06	669.72 ± 0.07	669.31 ± 0.05
FWHM	12.16 ± 0.15	12.80 ± 0.13	11.67 ± 0.11	12.02 ± 0.13	12.63 ± 0.13	13.15 ± 0.14	13.08 ± 0.10
	6.21 5.95	7.09 5.71	6.09 5.58	6.36 5.66	6.69 5.94	7.16 5.99	6.83 6.25
% area	19.89 ± 0.36	20.44 ± 0.35	20.62 ± 0.30	23.28 ± 0.39	28.96 ± 0.41	26.80 ± 0.47	29.09 ± 0.33
(4) λ_{max} (nm)	677.19 ± 0.06	677.40 ± 0.05	677.46 ± 0.04	677.93 ± 0.05	677.53 ± 0.05	677.71 ± 0.07	676.69 ± 0.05
FWHM	12.06 ± 0.12	12.10 ± 0.09	11.46 ± 0.08	10.68 ± 0.10	12.20 ± 0.09	13.38 ± 0.14	12.53 ± 0.09
	6.05 6.01	6.00 6.10	5.52 5.94	5.25 5.43	6.14 6.06	6.55 6.83	6.21 6.32
% area	22.85 ± 0.36	28.95 ± 0.42	24.97 ± 0.30	23.25 ± 0.37	29.68 ± 0.41	28.93 ± 0.49	28.93 ± 0.34
(5) λ_{max} (nm)	683.79 ± 0.08	682.70 ± 0.06	683.56 ± 0.06	684.42 ± 0.09	684.52 ± 0.06	683.83 ± 0.08	684.12 ± 0.05
FWHM	12.15 ± 0.18	12.61 ± 0.14	12.46 ± 0.14	11.43 ± 0.20	12.77 ± 0.08	14.70 ± 0.17	12.62 ± 0.13
	6.18 5.97	6.37 6.24	5.97 6.49	5.40 6.03	6.59 6.18	7.28 7.42	6.07 6.55
% area	14.37 ± 0.30	18.28 ± 0.33	15.62 ± 0.25	12.14 ± 0.30	20.23 ± 0.34	24.66 ± 0.46	18.89 ± 0.27
(6) λ_{max} (nm)	693.17 ± 0.30	692.80 ± 0.24	694.83 ± 0.18	694.95 ± 0.42	694.51 ± 0.22	696.65 ± 0.30	695.10 ± 0.17
FWHM	10.29 ± 0.64	13.45 ± 0.23	11.35 ± 0.44	11.47 ± 0.92	10.20 ± 0.34	13.66 ± 0.76	13.28 ± 0.46
	3.50 6.79	5.10 8.35	4.44 6.91	5.12 6.35	4.15 6.06	5.41 8.25	5.44 7.84
% area	1.50 ± 0.12	2.79 ± 0.41	1.96 ± 0.09	1.67 ± 0.17	2.18 ± 0.14	2.57 ± 0.17	3.06 ± 0.13

[a] The percentage areas of the spectral forms have been calculated, for each complex, from the total area given by the sum of all the bands. The FWHM is given as a left and a right value. The FWHM of each band is the sum of the two values. All the band parameters were left free in these fits. The errors for each of the fit parameters have been calculated as described under Materials and Methods.

Table II: Fractional Absorption of the Spectral Forms Present in Each chl–Protein Complex of the "Reconstituted" PS II Antenna[a]

spectral band (λ_{max}, nm)	LHCII	CP29	CP26	CP24	PS II core	$\sum B$
644		0.009				
648	0.123 (0.88)		0.011 (0.08)	0.006 (0.04)		0.140
660	0.106 (0.57)	0.011 (0.06)	0.011 (0.06)	0.006 (0.03)	0.053 (0.28)	0.187
670	0.111 (0.49)	0.014 (0.06)	0.013 (0.06)	0.007 (0.03)	0.081 (0.36)	0.226
678	0.128 (0.50)	0.020 (0.08)	0.016 (0.06)	0.007 (0.03)	0.083 (0.33)	0.254
684	0.080 (0.49)	0.013 (0.08)	0.010 (0.06)	0.004 (0.02)	0.058 (0.35)	0.164
695	0.008 (0.47)	0.002 (0.12)	0.001 (0.06)		0.006 (0.35)	0.017
$\sum A$	0.556	0.069	0.062	0.030	0.280	
[chl $a+b$]	0.616	0.066	0.059	0.033	0.232	

[a] The numbers in parentheses are the fractional absorptions of the spectral forms of each complex with respect to the total absorption of that spectral form in the "reconstituted" PS II antenna. $\sum B$ is the absorption of each spectral form in the "reconstituted" antenna and was obtained by summing the fractional absorption values of the individual spectral forms in the different complexes. $\sum A$ is the absorption of each complex in the "reconstituted" antenna and was obtained by summing the fractional absorption values of the various spectral forms in each complex. [chl $a+b$] represents the stoichiometric concentrations of chl a plus chl b in the different complexes.

From Table II, several interesting points emerge: (1) The absorption (Q_y transition) of each of the antenna complexes can be calculated ($\sum A$ of Table II) and compared with the stoichiometric chlorophyll data of Dainese and Bassi ([chl $a+b$]). Thus, it can be seen that the LHCII absorption is about 10% less than the corresponding chlorophyll concentration value whereas the PS II core absorption is about 20% higher than the chl concentration value. These differences are due to the presence of chl b, which has a lower Q_y extinction coefficient than chl a (Zucchelli et al., 1990), in LHCII and not in the PS II core. (2) With the exception of the 660-nm spectral form, the chl a forms are somewhat enriched in the core antenna and slightly impoverished in LHCII. This is also due to the presence of chl b in LHCII and its absence from the PS II core.

Calculation of the Equilibrium Distribution of Excited States between PS II chl–Protein Complexes. On the basis of the data in Table II, one can calculate the absorption population weighted equilibrium distribution of excited states among the spectral forms using the Boltzmann distribution $N_i/N_j = (g_i/g_j)\exp(-\Delta_{ij}/kT)$, where N_i/N_j is the equilibrium excited-state ratio of spectral forms i and j with energy separation Δ_{ij}, g_i/g_j is the absorption population weighting term, k is the Boltzmann constant, and T is the absolute temperature. The main assumption of this approach is that the relative areas under the Gaussian bands represent appropriate weighting factors. Thus, the bands should be substantially symmetical around their representative energy levels, as is the case. This calculation was initially performed for the total antenna data ($\sum B$ of Table II). Subsequently, values were assigned to the individual spectral forms within each complex by employing the appropriate absorption population weighting factor. The calculated data are presented in Table III. By summing the equilibrium values for each of the spectral forms comprising a chl–protein complex, one determines the equilibrium distribution of excited states associated with each complex within the "reconstituted" PS II antenna (Table III). Thus, it is seen that at equilibrium about half the excited states in PS II antenna are expected to be associated with LHCII and about one-third with the core antenna. The remaining 16% are distributed between the three minor chl–protein complexes. It is interesting to note that these calculated excited-state distribution values are very similar to the stoichiometric values for chl a in the

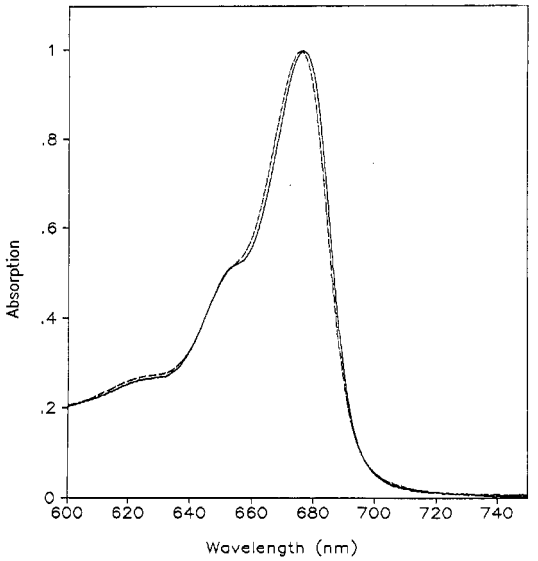

FIGURE 4: Comparison between the measured absorption spectrum of PS II membranes from maize (full line) and the calculated absorption spectrum of the "reconstituted" PS II antenna (dashed line). See text for details of the calculation procedure.

complexes (LHCII, 0.51; PS II core, 0.33; CP29, 0.07; CP26, 0.06; CP24, 0.03; see Discussion).

The equilibrium excited-state distribution for the two principal PS II core antenna complexes, CP47 and CP43, has also been calculated (Table III) assuming equal chl *a* binding for these two complexes, which together constitute about 90% of the total core chl (Dainese & Bassi, 1991). As can be seen, excitation energy is predicted to equilibrate almost equally between them.

DISCUSSION

In the present paper, we examine the distribution of the chl spectral forms between the various chl–protein complexes. It is shown that only in the case of chl *b* is there a markedly asymmetric distribution between external antenna complexes and the core antenna. The short-wavelength chl a^{660} is slightly enriched in LHCII with respect to the other chl *a* forms and is present at somewhat reduced levels in the core. This confirms a previous observation (Jennings et al., 1990). In the well-known "funnel" model of PS II antenna, it is expected that the long-wavelength spectral forms (chl^{684} and chl^{695}) should be significantly concentrated near the RCs, i.e., in the core antenna. We find no evidence for such a distribution. In this context, the presence of a quite strong transition near 684 nm in LHCII is important as, according to the present analysis, about half the total chl^{684} is associated with this complex. On the basis of a low-temperature analysis of dodecyl maltoside solubilized LHCII, Hemelrijk et al. (1992) have suggested that this band is absent in LHCII. Evidence has, however, been presented suggesting that the 684-nm band in LHCII is temperature-sensitive, being substantially reduced at low temperatures (Zucchelli et al., 1990). Thus, we believe that the failure of these authors to detect this transition may be attributable to their experimental conditions. Additional support for the presence of chl^{684} in LHCII comes from our recent demonstration that a Gaussian fluorescence band, present at high levels in LHCII and peaking at 687 nm, can be ascribed to this spectral form. The 687-nm emission band is drastically decreased upon lowering the temperature to 77 K (unpublished observation).

As mentioned in the introduction, small differences in the RC trapping efficiency for the spectral forms have been demonstrated by steady-state fluorescence excitation and emission techniques (Jennings et al., 1990, 1991). Thus, one can write the following relative trapping efficiency sequence for PS II:

$$chl^{684}_{687} > chl^{678}_{680} > chl^{670}_{672} > chl^{660}_{663} > chl^{648}_{652}$$

While the relatively low trapping efficiency for chl^{648} and chl^{660} may be associated with their topological distribution in the PS II antenna, i.e., their presence at higher levels in the outer antenna with respect to the core antenna, a similar explanation does not seem tenable for the high trapping efficiency of chl^{684}.

On the basis of the relative absorption of the chl spectral forms in the antenna complexes, it has been possible to calculate the expected equilibrium distribution of excited states within the PS II antenna using the Boltzmann distribution expression. Thus, we find that at equilibrium about one-third (36%) of the excited states are associated with the core antenna, and are approximately equally distributed between CP47 and CP43. Approximately half (49%) are associated with LHCII and the remaining 17% with the minor antenna complexes CP24, CP26, and CP29. These data permit a definite conclusion to be reached on the so-called "funnel" model of PS II antenna. In this context, it is interesting to compare the excited-state distribution data for the core complex (33.9%) with its relative light absorption capacity (28%). The ratio of these two parameters (33.9/28 = 1.21) gives a good idea of the "funnel" capacity of the core antenna. The analogous term for LHCII is 0.88 with intermediate values for the three minor complexes. Thus, the PS II antenna may be considered to be organized as a very shallow funnel.

If one considers the core antenna–outer antenna equilibrium for excited states:

$$A^*_{ext} + A_{core} = A^*_{core} + A_{ext}$$

one finds $K_{eq} = 1.32$. According to $\Delta G = -RT \ln K_{eq}$ (G is the standard Gibbs free energy, R is the gas constant, T is the absolute temperature, and K_{eq} is the equilibrium constant), the free energy change associated with excited-state transfer from the external antenna to the core antenna at room temperature is –0.17 kcal mol^{-1}. This is a small value, being considerably less than the thermal energy (RT), and is indicative of the extremely shallow nature of the PS II antenna funnel. In this context, it is interesting to note that Owens et al. (1988) have concluded, on the basis of picosecond fluorescence studies and absorption Gaussian band analyses, that the spectral forms in the photosystem I core antenna are rather homogeneously distributed with respect to the RC. It would therefore seem that the "funnel" organization of the chlorophylls in higher plant photosystems is limited and does not play a major role in energy trapping.

As noted under Results, the equilibrium excited-state distribution terms of the complexes (LHCII, 0.49; CP29, 0.08; CP26, 0.06; CP24, 0.03; core, 0.34) are very similar to the relative stoichiometries for chl *a* (LHCII, 0.51; CP29, 0.07; CP26, 0.06; CP24, 0.03; core, 0.33). This indicates that the slight funnel effect is not due to spectral forms of chl *a* but is caused exclusively by the asymmetric distribution of chl *b* between outer and core antenna.

As discussed above, on the basis of the thermodynamic equilibrium assumption we have determined the expected excited-state distribution between the chl–protein complexes in PS II antenna. This information is useful in understanding energy transfer within PS II. However, it is interesting to consider whether equilibrium is effectively attained within

Table III: Calculated Equilibrium Excited-State Distribution Values for Each Spectral Form Present in the Different chl–Protein Complexes of the "Reconstituted" PS II Antenna[a]

spectral band (λ_{max}, nm)	LHCII	CP29	CP26	CP24	PS II core	CP47	CP43
648	0.006						
660	0.019	0.002	0.002	0.001	0.010	0.004	0.004
670	0.060	0.008	0.007	0.004	0.044	0.018	0.020
678	0.161	0.025	0.020	0.009	0.104	0.045	0.045
684	0.188	0.030	0.023	0.009	0.135	0.063	0.055
695	0.059	0.014	0.009	0.004	0.046	0.023	0.028
[S]	0.493	0.079	0.061	0.027	0.339	0.153	0.152

[a] For details of the calculation procedure, see the text. For these calculations, the "reconstituted" antenna comprised LHCII, PS II core, CP24, CP26, and CP29. The excited-state equilibria between CP43 and CP47 have been calculated separately. [S] is the excited-state concentration in each chl–protein complex and was obtained by summing the values for the individual spectral forms within each of the different complexes.

Table IV: Comparison between the Normalized Contribution of the chl Spectral Forms to the Emission Spectrum of BBY-grana with That Calculated Using the Boltzmann Distribution Expression[a]

spectral form (λ_{max}, nm)	Boltzmann factor	numerical decomposition of emission spectra	
		RCs open	RCs closed
648	0.01	0.02	0.02
660	0.04	0.05	0.05
670	0.13	0.15	0.16
678	0.31	0.34	0.36
684	0.31	0.31	0.33
695	0.21	0.09	0.09

[a] The data have been taken from Zucchelli et al. (1992). The Boltzmann values have been calculated from the λ_{max} of the BBY-grana absorption bands using the absorption band at 684 nm as reference and the relative areas under the absorption bands as weighting factors. The temperature was 300 K.

PS II antenna prior to trapping. One way of examining this is to analyze the steady-state distribution of excited states between the chl spectral forms by determining the areas under the Gaussian emission bands associated with the chl spectral forms. This approach has been used with success for isolated LHCII (Zucchelli et al., 1992) where it was shown that, to a first approximation, a Boltzmann equilibrium of excited states between the spectral forms is attained. In Table IV, a similar analysis to that previously performed for LHCII (Zucchelli et al., 1992) is presented for the BBY-grana preparation, using previously published data (Zucchelli et al., 1992). The experimentally determined excited-state distribution based on the fluorescence emission bands is presented for BBY-grana with RCs either fully closed or partially open. It is seen that there is a reasonably close correspondence between the calculated and the measured values for the excited-state distribution between the spectral forms for all forms except the minor long-wavelength chl[695]. In this case, the calculated value is considerably greater than the measured one. We feel that such a discrepancy, which is not present in isolated LHCII (Zucchelli et al., 1992), may be due to an overestimation of the absorption contribution of this minor band which is present in the long-wavelength tail of the absorption spectrum where it constitutes about 2% of the total Q_y absorption according to Gaussian decomposition analysis (Zucchelli et al., 1992). Such an overestimation could be introduced in BBY-grana and not in LHCII as only the former preparation requires the application of a light-scattering correction. If this correction were to be slightly underestimated, it would lead to a relatively large overestimation of this absorption form compared with the others. This would result in a proportional increase in the calculated excited-state density associated with this form. It is therefore concluded that, with the possible exception of the minor chl[695] spectral form, the excited-state distribution between the spectral forms is reasonably well described by a Boltzmann equilibrium at either open or closed RCs. This conclusion, which is in substantial agreement with that of McCauley et al. (1989) using picosecond fluorescence decay analysis techniques, is important as it suggests that the calculated equilibrium excited-state distribution between the PS II antenna complexes presented in this paper probably closely approximates that which exists normally within PS II.

As indicated above, the data presented in this study are not in favor of exciton transfer within the PS II antenna being strongly directed toward RCs. Energy seems to be distributed between the various chlorophyll–protein complexes largely according to their chl *a* content. This conclusion therefore raises the interesting question of why the PS II antenna should have such a high level of structural complexity. In this context, the role of the minor complexes (CP24, CP26, CP29) is particularly intriguing. Since the number of chl molecules associated with these complexes is low (about 16% of total antenna absorption), their principal function does not seem to be that of increasing the absorption cross section of PS II. Biochemical data suggest that they seem to connect the major antenna complex, LHCII, to the core antenna (Bassi et al., 1987; Dainese & Bassi, 1991; Peter & Thornber, 1991) and therefore that they may act as a kind of "bridge" for energy transfer from LHCII to the core. While the present study of the equilibrium excited-state distribution based on spectroscopic characteristics indicates that they are well enough suited for such a role from an energetic point of view, in this respect they are not very different from either LHCII or the core complexes. Thus, it is difficult to envisage their presence only in terms of a "bridge" function for energy transfer. An interesting possibility is that the minor chlorophyll–protein complexes may have a regulatory function in terms of energy transfer to the core antenna. This possibility is supported by recent results which suggest that the minor complexes are involved in (a) complex–complex interactions during state I–state II transitions (Bassi & Dainese, 1992) and (b) the dissipation of excitation energy into heat through nonphotochemical quenching since zeaxanthin and its precursors violaxanthin and antheraxanthin (Demmig et al., 1987) are located in CP24, CP26, and CP29 (Dainese et al., 1993).

In the present paper, we have analyzed the expected equilibrium excited-state distribution within the chl–protein complexes associated with the PS II antenna using the technique of Gaussian band decomposition of the main Q_y absorption transitions. While there is good general agreement that this technique describes a number of separate electronic transitions associated with different chl spectral forms, in the context of the present study it may be viewed as a convenient way of dividing up the red chl absorption band into different energy levels, each with a weighting parameter. Thus, the overall validity of our conclusions concerning excited-state

distribution at equilibrium is not limited by the commonly made assumptions associated with the Gaussian analysis.

ACKNOWLEDGMENTS

We thank Dr. O. Cremonesi for helpful discussions on the curve-fit analysis.

REFERENCES

Anderson, J. M. (1980) *Biochim. Biophys. Acta 591*, 113–126.
Anderson, J. M. (1986) *Annu. Rev. Plant Physiol. 37*, 93–136.
Bassi, R., & Simpson, D. J. (1986) *Carlsberg Res. Commun. 51*, 363–370.
Bassi, R., & Dainese, P. (1992) *Eur. J. Biochem. 204*, 317–326.
Bassi, R., Hoyer-Hansen, G., Barbato, R., Giacometti, G. M., & Simpson, D. J. (1987) *J. Biol. Chem. 262*, 13333–13341.
Bassi, R., Rigoni, F., & Giacometti, G. (1990) *Photochem. Photobiol. 52*, 1187–1206.
Berthold, D. A., Babcock, G. T., & Yocum, C. F. (1981) *FEBS Lett. 134*, 231–234.
Bevington, P. R. (1969) *Data Reduction and Error Analysis for the Physical Sciences*, McGraw-Hill, New York.
Brown, J. S., & Schoch, S. (1981) *Biochim. Biophys. Acta 636*, 201–209.
Dainese, P., & Bassi, R. (1991) *J. Biol. Chem. 266*, 8136–8142.
Dainese, P., Hoyer-Hansen, G., & Bassi, R. (1990) *Photochem. Photobiol. 51*, 693–703.
Dainese, P., Marquardt, J., Pineau, B., & Bassi, R. (1993) in *Research in Photosynthesis*, Vol. 1, pp 287–290, Kluwer, Dordrecht, The Netherlands.
Dekker, J. P., Bowlby, N. R., & Yocum, C. F. (1989) *FEBS Lett. 254*, 150–154.
Demmig, B., Winter, K., Kruger, A., & Czygan, F.-C. (1987) *Plant Physiol. 84*, 218–224.
Di Paolo, M. L., Peruffo dal Belin, A., & Bassi, R. (1990) *Planta 181*, 275–286.
Dunahay, T. G., Staehelin, L. A., Seibert, M., Ogilvie, P. D., & Berg, S. P. (1984) *Biochim. Biophys. Acta 764*, 170–193.
Duysens, L. N. M. (1956) *Biochim. Biophys. Acta 19*, 1–12.
Fling, S. P., & Gregerson, D. S. (1986) *Anal. Biochem. 155*, 83–88.
French, C. S., Brown, J. S., & Lawrence, M. C. (1972) *Plant Physiol. 49*, 421–429.
Ghanotakis, D. F., Demetriou, D. M., & Yocum, C. F. (1987) *Biochim. Biophys. Acta 891*, 15–21.
Gillbro, T., Sandstrom, A., Spangfort, M., Sundstrom, V., & Van Grondelle, R. (1988) *Biochim. Biophys. Acta 934*, 369–376.
Hemelrijk, P. W., Kwa, S. L. S., Van Grondelle, R., & Dekker, J. P. (1992) *Biochim. Biophys. Acta 1098*, 159–166.
Jennings, R. C., Islam, K., & Zucchelli, G. (1986) *Biochim. Biophys. Acta 850*, 484–489.
Jennings, R. C., Zucchelli, G., & Garlaschi, F. M. (1990) *Biochim. Biophys. Acta 1016*, 259–265.
Jennings, R. C., Zucchelli, G., & Garlaschi, F. M. (1991) *Biochim. Biophys. Acta 1060*, 245–250.
Kyle, D. J., Kuang, T.-Y., Watson, J. L., & Arntzen, C. J. (1984) *Biochim. Biophys. Acta 765*, 89–96.
Latimer, P. (1983) *Photochem. Photobiol. 38*, 731–734.
Leibl, W., Breton, J., Deprez, J., & Trissl, H.-W. (1990) in *Current Research in Photosynthesis* (Baltscheffsky, M., Ed.) Vol. 2, pp 305–308, Kluwer, Dordrecht, The Netherlands.
McCauley, S. W., Bittersmann, E., & Holzwarth, A. R. (1989) *FEBS Lett. 249*, 285–288.
Nanba, O., & Satoh, K. (1987) *Proc. Natl. Acad. Sci. U.S.A. 84*, 109–118.
Owens, G. T., Webb, S. P., Alberte, R. S., Mets, L., & Fleming, G. R. (1988) *Biophys. J. 53*, 733–745.
Peter, G. F., & Thornber, J. P. (1991) *J. Biol. Chem. 266*, 16745–16754.
Porra, R. J., Thompson, W. A., & Kriedermann, P. E. (1989) *Biochim. Biophys. Acta 975*, 384–394.
Reddy, N. R. S., Lyle, P. A., & Small, G. J. (1992) *Photosynth. Res. 31*, 167–194.
Shipman, L. L., Cotton, T. M., Norris, J. R., & Katz, J. (1976) *J. Am. Chem. Soc. 98*, 8222–8230.
Smith, K., Krohn, R. I., Hermanson, G. T. Mallia, A. K., Gartner, F. H., Provenzano, O., Fujimoto, E. K., Goeke, N. M., Olsen, B. J., & Klenk, D. C. (1985) *Anal. Biochem. 150*, 76–85.
Spangfort, M., & Andersson, B. (1989) *Biochim. Biophys. Acta 977*, 163–170.
Van Dorssen, R. J., Breton, J., Plijter, J. J., Satoh, K., Van Gorkom, H. J., & Amesz, J. (1987a) *Biochim. Biophys. Acta 893*, 267–274.
Van Dorssen, R. J., Plijter, J. J., Dekker, J. P., Den Oude, A., Amesz, J., & Van Gorkom, H. J. (1987b) *Biochim. Biophys. Acta 890*, 134–143.
Van Ginkel, G., & Kleinen-Hammans, J. W. (1981) *J. Photochem. Photobiol. 31*, 385–395.
Wellburn, A. R., & Lichtentaler, H. K. (1983) in *Advances in Photosynthesis Research* (Sybesma, C., Ed.) Vol. II, pp 10–12, Martinus Nijhof Publishers, Dordrecht, The Netherlands.
Zucchelli, G., Jennings, R. C., & Garlaschi, F. M. (1990) *J. Photochem. Photobiol. B: Biol. 6*, 381–394.
Zucchelli, G., Jennings, R. C., & Garlaschi, F. M. (1992) *Biochim. Biophys. Acta 1099*, 163–169.